

D. Borodin, M. Stamp, A. Kirschner, C. Björkas, S. Brezinsek, J. Miettunen,
D. Matveev, C. Silva, O. Van Hoey, M. Groth, S. Marsen, V. Philipps
and JET EFDA contributors

Spectroscopic Measurements of Be Erosion at JET ILW and Interpretation with ERO Modelling

“This document is intended for publication in the open literature. It is made available on the understanding that it may not be further circulated and extracts or references may not be published prior to publication of the original when applicable, or without the consent of the Publications Officer, EFDA, Culham Science Centre, Abingdon, Oxon, OX14 3DB, UK.”

“Enquiries about Copyright and reproduction should be addressed to the Publications Officer, EFDA, Culham Science Centre, Abingdon, Oxon, OX14 3DB, UK.”

The contents of this preprint and all other JET EFDA Preprints and Conference Papers are available to view online free at www.iop.org/Jet. This site has full search facilities and e-mail alert options. The diagrams contained within the PDFs on this site are hyperlinked from the year 1996 onwards.

Spectroscopic Measurements of Be Erosion at JET ILW and Interpretation with ERO Modelling

D. Borodin¹, M. Stamp, A. Kirschner¹, C. Björkas^{1,3}, S. Brezinsek¹, J. Miettunen⁴,
D. Matveev¹, C. Silva⁵, O. Van Hoey⁶, M. Groth⁴, S. Marsen⁷, V. Philipps¹
and JET EFDA contributors*

JET-EFDA, Culham Science Centre, OX14 3DB, Abingdon, UK

¹*Institute of Energy and Climate Research - Plasma Physics, Forschungszentrum Jülich GmbH,
Association EURATOM-FZJ, Partner in the Trilateral Euregio Cluster, Jülich, Germany*

²*EURATOM-CCFE Fusion Association, Culham Science Centre, OX14 3DB, Abingdon, OXON, UK*

³*EURATOM-Tekes, Department of Physics, P.O. Box 43, FI-00014 University of Helsinki, Finland*

⁴*Aalto University, EURATOM-Tekes, Espoo, Finland*

⁵*Associação Euratom/IST, Instituto de Plasmas e Fusão Nuclear, Instituto Superior Técnico, Lisbon, Portugal*

⁶*Department of Applied Physics, Ghent University, Rozier 44, 9000 Ghent, Belgium*

⁷*Max-Planck-Institut für Plasma Physics, EURATOM Association, Greifswald, Germany*

** See annex of F. Romanelli et al, "Overview of JET Results",
(23rd IAEA Fusion Energy Conference, Daejeon, Republic of Korea (2010)).*

Preprint of Paper to be submitted for publication in Proceedings of the
20th International Conference on Plasma Surface Interactions , Eurogress, Aachen, Germany
21st May 2012 - 25th May 2012

ABSTRACT

Beryllium (Be) erosion has been studied in dedicated limiter discharges in JET with the recently installed ITER-like wall [7]. Passive spectroscopy [1] in the vicinity of the solid Be limiter is used for measurement of the Be physical sputtering as the main erosion mechanism. To consider the 3D configuration of plasma parameters and electromagnetic field, actual limiter shape and local transport affecting the fraction of Be coming into the observation volume, detailed modelling with the ERO code has been applied to interpret the experimental data. The observed dependence of line intensities and line ratios on plasma parameters during the density scan and various line ratios are used to validate the model and the underlying data including the recently introduced assumptions for Be physical sputtering, the very same which were used before for ITER predictive modelling [2].

INTRODUCTION

The erosion of beryllium (Be) determines the life time of first wall components in fusion devices such as the ITER Blanket Modules (BM), the Be influx into the plasma (dilution) and affects tritium retention due to co-deposition. The 3D Monte-Carlo (MC) impurity transport and plasma-surface interaction code ERO was successfully applied for simulation of the ITER BM life time and compared with earlier LIM calculations [2] as well as for the ITER divertor duty cycle, mostly limited by the retention [11]. For instance, it was shown that the uncertainties (sec.2, tab.1) in the physical sputtering data lead to BM life time estimations varying within factor 4. Therefore, an assessment of Be sputtering at existing experiments is of great importance. In particular it is important to validate the models and underlying data at the JET ITER-like wall [7], which has a similar complicated power-load optimised geometry as ITER BM in combination with similar 3D configuration of plasma and electromagnetic field. The same ERO code also is continuously applied to erosion experiment at PISCES-B [4] – a linear device, one of the few ITER-relevant plasma experiments allowing operation with toxic Be.

The focus of this paper is Be erosion measurements using the passive spectroscopy at JET ILW during the plasma density scan. The limiter plasmas used in this experiment are suitable for assessing of Be erosion, as it is significantly larger than in the divertor regime. In addition, limiter plasmas are relevant for ITER start-up phase. The spectroscopic system registers specially integrated light in the vicinity of solid shaped Be limiter. It provides time-resolved simultaneous registration of several BeI, BeII and D (deuterium) lines. The line emission can be converted into the respective particle fluxes using S/XB factors [12] provided by ADAS [5]. The ratio of Be and D fluxes gives an estimate for an effective sputtering yield, which is assumed to be the main erosion mechanism. The precision of spectroscopic measurements as well as S/XB values is about 20%.

However, an effective yield includes an additional erosion due to self-sputtering by Be contained in the plasma, local geometry and other factors pertaining to the actual experiment. The sputtering yield is known to have dependence on incident energy and angle [3]. Plasma particles impact with certain distributions of these parameters, which are unique for every surface point due to complex

limiter shape and varying plasma parameters. Thus, interpretation of the measured effective yield and its extrapolation for ITER is an elaborate.

Therefore, to obtain the sputtering yield, which is invariant for all experimental situations a detailed 3D modelling is necessary for example by ERO code mentioned above. MC simulations allow reproducing the line emission observed assuming sputtering yield as a given function, though it is difficult to use such approach for solution of the reverse problem – to get a yield from the light. Therefore, we use high and low estimates (sec. 2) for the yield deduced on the basis of various simulated data in the form of the recent fit [3] and aim to prove that existing experiments confirm these limits. This is a first ERO application to the situation at hand, therefore the main aim of the current stage was to test the model reasonability by reproducing of the observed Be line intensities and also their ratios varying during the plasma density scan as a benchmark for ERO simulations.

1. EFFECTIVE YIELD MEASUREMENT

The general geometry is illustrated in fig.1. The observation system is directed on the solid Be tile #7 of the octant 7X of the JET inner wall as is shown in fig.1 b). Figure 1 a) shows the tile position inside the poloidal cross-section of JET. The tile is positioned in the scrape-off-layer (SOL) several cm away from the separatrix. The line of sight (“spot”) is nearly cylindrical with radius of about 60mm and directed at 58° to the torus radius taken at the limiter centre tipz axis (which is parallel to the JET coordinate RC). The spectroscopic system registers the total light emitted inside the observation volume. It is equipped with a survey spectrometer equipped with a CCD camera number of narrow-band filters providing time-resolved simultaneous registration in the visual range of several BeI, BeII, D lines and also BeD molecular band. The ERO coordinate system is used, which is explained in sec 3.

The plasma parameters (electron density and temperature) are measured by the reciprocating probe [14] at the top of the device and mapped [10] in the poloidal plane using the 2-point model. Fig. 1 (c, d) shows the poloidal cross-section of the plasma density together with a limiter contour. Toroidal symmetry is assumed to get the 3D picture just by rotation of the 2D map around the torus axis (parallel to B-field). As an example toroidal cross-section of electron density is given in fig.1e. The mapping was carried out for 2 discharges corresponding to upstream line-averaged densities (interferometer, JET signal ‘KG1L/LAD3’) of $3.7 \times 10^{19} \text{ m}^{-2}$ and $8 \times 10^{19} \text{ m}^{-2}$. The same measurement was used for linear interpolation of the mapped plasma parameters for any time point of the entire density scan (sec. 3). In general, electron density and temperature near the limiter surface during the scan were of the order of $T_e \sim 10 \div 30 \text{ eV}$, $n_e \sim 1 \div 2 \times 10^{12} \text{ cm}^{-3}$.

The most straightforward way to interpret the experiment for sputtering yields is to use the S/XB values [12] to convert the photon fluxes of D and Be species into the respective particle fluxes. The ratio of the D and Be fluxes gives the effective yield, which includes both sputtering by plasma ions and Be impurities. For instance assuming as a crude estimation that all eroded Be comes back to the same location the effective yield $Y_{\text{eff}} = Y_{\text{DBe}} / (1 - Y_{\text{BeBe}})$, where Y_{DBe} and Y_{BeBe} are respectively Be

sputtering yields by D plasma and Be impurity. This method gives effective Be sputtering yields about 10% or somewhat smaller in the large range of plasma parameters applied for limiter plasmas used for the erosion study.

The precision of both spectroscopic measurements and S/XB values is quite high, about 20%. However, the resulting effective yield is result of the interplay of various physical effects in context of complicated geometry. Therefore, for correct interpretation of experiment and separation of universal parameters, which can be extrapolated for ITER, a detailed modelling of Be erosion, local transport and light emission described in sec. 3 is necessary.

2. PHYSICAL SPUTTERING MODEL AND DATA

The available in literature empirical and various simulated sputtering yields (fig. 2) can differ by orders of magnitude [8,9]. At that the simulated data shows less scattering and, more important, follows similar trends allowing to fit it as function of incident ion energy and angle. In our view, the deviations of empirical data are often not because of measurement techniques, but rather due to the complications of an interpretation of the observed effective yields as universal values. For instance, in most plasma experiments it is difficult to separate the angular dependence as an averaged erosion picture is observed.

Therefore, ERO uses a comprehensive approach for sputtering yields Y in the form of a recent fit [3] depending on impact energy E_{in} and angle α_{in} in the factorized form $Y(E_{in}, \alpha_{in}) = Y(E_{in}, 0) * A(E_{in}, \alpha_{in})$. For the normal incidence part $Y(E_{in}, 0)$ we use high “ERO-max” and low “ERO-min” limit fits (table 1) deduced on the basis of simulations by SDTrimSP (MC, based on binary-collision approximation) and Molecular Dynamics (MD) with various assumptions. E.g. the lower yields are to a large extent determined by the assumption of 50% D concentration in the surface. Fig. 2 presents the data points from SDTrimSP and MD calculations and resulting fits of high and low Be sputter yields by D impact at normal incidence. Be by Be self-sputter case is similar. For the angular part $A(E_{in}, \alpha_{in})$ just SDTrimSP simulations for pure Be and 50% D surface concentration in Be are used.

By tracking impurity particles eroded according to the assumed yields Monte-Carlo simulations allow to simulate respective light emission patterns. The restoration of the yield from the light would demand additional assumptions.

In general, for erosion by background D plasma and intrinsic impurity ions the pre-calculated distributions of E_{in} and angle α_{in} for respective particles should be used for every surface cell to obtain the averaged sputtering yield. Thus, the high “ERO-max” and low “ERO-min” fits $Y(E_{in}, \alpha_{in})$ are universal for any experiment at hand. For testing purposes ERO can use more simple assumptions, e.g. one can assume normal incidence with the energy determined as a sum of thermal component $\sim 2T_i$ and sheath potential $\sim 3Z * T_e$, where T_i , T_e are local ion and electron temperatures and Z is the charge of impinging ion.

3. ERO SIMULATIONS OF THE DENSITY SCAN EXPERIMENT

Fig.1 illustrates the ERO simulation box and coordinate system. The axis x (toroidal) is chosen to be perpendicular to the torus radius at the shaped limiter central tip. The z-axis is chosen perpendicular to x in the toroidal plane (parallel to the JET coordinate 'RC'). This makes it nearly perpendicular to the limiter surface. The orthogonal to x and z coordinate y is parallel to torus axis (JET 'ZC'). The spectroscopic system line of sight is nearly cylindrical with radius of about 60mm and directed at 58° to the z axis. The simulation box covers small area of neighbour tiles 6 and 8, which are included in the simulation box because particles eroded from these surfaces can be transported into the spot volume.

ERO simulates the 3D photon emission patterns of Be species using the simulated trajectories to calculate density at every location, which is then multiplied with a photon emission coefficient (PEC) from ADAS [5] depending on local plasma parameters. Then the total light emitted inside the experimental observation volume is integrated. One also can integrate the 3D light pattern along any line of sight to simulate the respective perpendicular 2D view as it could be seen in an experiment. Fig. 3 shows integrated in y-direction light patterns (a toroidal view) of Be species. Even the pattern of neutral BeI is quite non-trivial as particles are eroded inhomogeneously along the surface and get ionized at certain locations depending on the plasma parameter along their trajectory. Their light is also dependent on local plasma parameters. The BeII emission is even more complicated as Be^+ ions are driven by electromagnetic field, plasma flow, etc.

The S/XB approach (sec.1) implies that all particles are getting ionized inside the observation volume. It is also important that particles eroded far away can still be transported into the spot and contribute to the emission (fig.3). ERO tracks the eroded Be, therefore it can calculate erosion pattern along the surface, location of ionizations and, finally, the amount of species coming into the spot from the whole limiter surface. The last varies with plasma parameters. The ionizations rates and PEC used by ERO come as well as S/XB from ADAS [5].

An additional issue is that the erosion of Be along the limiter surface depends on multiple parameters. The inclination of the surface to magnetic field determines the impinging D flux, the local effective yield depends on local plasma parameters in the vicinity etc. Fig.4 shows 2 resulting erosion patterns simulated by ERO for various densities. They are essentially different, which affects the fraction of locally eroded Be species coming into the spot.

The total light of several BeI and BeII lines inside the spot was registered during the scan of the plasma line-averaged density. Fig.5 shows BeII 527nm line as an example. We assume a certain relation between the plasma parameter radial dependence near the plasma edge (reciprocating probe) and the line-averaged upstream density along a chord of torus. For the first modelling attempt the linear interpolation of mapped plasma parameters between two density points indicated on fig.5 were used. The plasma parameter simulations for instance by SOLPS [13], which provides also the input for the ITER simulations [2], or other 2D or even 3D models could help to understand this relation better. It is also possible to improve in future the situation from the empirical side by

combining further diagnostics in addition to the reciprocating probe, by providing mapping for more than 2 points etc.

The concentration of Be impurity is estimated from the effective charge Z_{eff} measurements. At high density Z_{eff} becomes close to 1, which means that Be concentration is negligible, however at low density it is quite significant. For example at $4 \times 10^{19} \text{ m}^{-2}$ the concentration can be estimated to be 8.5% assuming all Be comes to the limiter as Be^{4+} and 17% assuming it comes as Be^{3+} . To achieve maximal self-sputtering effect in the modelling the following extreme assumptions are taken: all Be impurity is in Be^{3+} ionization state and Be self-sputtering yield is multiplied by 2 to account for possible data uncertainties. This allows to nearly reproduce by ERO simulations the observed slope (fig.5) for the BeII 527nm line intensity growing with electron density. The role of self-sputtering increases towards low densities. The situation for BeI 457nm is similar.

At low electron densities below ‘low line-averaged density’ $3.7 \times 10^{19} \text{ m}^{-2}$ (outside ERO the mapped plasma interpolation range) and the same time higher electron temperatures the Z_{eff} indicated extremely high concentrations of Be, which is quite understandable as the sputtering yield grows with incident energy largely determined by sheath potential and this is synergistically strengthened by self-sputtering. It is interesting to note the opposite trend of liner intensity in that region observed in experiment.

Another possibility to benchmark the model is to compare line ratios. Fig. 6 demonstrates good agreement between ERO and experiment for line ratios inside BeII as well as for line ratios between two ionization states. It should be noted that the ratios are obviously little affected by Be erosion (only by the pattern geometry). Thus, they characterize the agreement with respect to Be transport simulation and also quality of atomic data used. The agreement for BeI/BeII ratios is slightly worse as they are affected by more uncertainties for instance the initial population of quasi-metastable BeI $1s^2 2s 2p \ ^3P$ state in comparison to the $1s^2 2s^2 \ ^1S$ ground state just after the sputtering. This population determines to a large extent the ratios between triplet and singlet lines and also affects ionization.

The difference between assumed limit estimates of Be sputtering yields (sec. 2) are mostly within factor 3-4. Despite the described modelling improves experiment interpretation, its accuracy is not enough to make judgement concerning the sputtering data quality. In any case it is clear that self-sputtering simulations based on Z_{eff} -based concentrations and the input plasma parameters mapped and interpolated in the described way can be used only for understanding of the qualitative picture and testing of the modelling reasonability, which was the aim of the current work stage.

Many physical effects were neglected. The formation of Be hydride molecules (Be-D) recently introduced in ERO [6] can be an additional erosion mechanism (MD data available). It is interesting to note the BeD light was observed in the same experiment. The self-sputtering treatment can be refined e.g. by assuming a certain profile of Be concentration at the plasma boundary in spite of a constant value.

SUMMARY

The passive spectroscopy is successfully used for erosion assesment of shaped solid Be limiter of recently installed JET ILW [7]. Physical sputtering is assumed to be the main erosion mechanism. Effective yields of about 10% and smaller observed for a wide range of plasma parameters in the series of limiter discharges especially aimed for erosion study.

The universal interpretation of the experiment resulting in invariant sputtering yields demands detailed modelling including interplay of multiple physical effects in the context of the complicated limiter geometry and 3D configuration of electromagnetic field and plasma parameter distribution. The ERO code is applied, which can be used to extrapolate the obtained erosion data for ITER first wall predictive modelling [2]. The modelling necessity for the interpretaion is confirmed by local transport modelling results.

The evolution of line intensities during the plasma density scan and the line ratios are used for model and underlying data benchmark. The ERO simulations reproduce general trend of growing with plasma density line intensities and absolute spectral lines ratios within factor 2 for BeII and BeI lines and even better for lines inside a single ionization state. This benchmark, which was main aim of the current work stage, indicates modelling reasonability.

The plasma parameters (ERO input) are the main source of uncertainties. The ERO modelling can be refined by taking other effects into account for instance more detailed treatment of self-sputtering by Be plasma impurity, Be-D molecule release, which can serve as an additional erosion mechanism and adjusting metastable population. One more issue is uncertainties in the aatomic data.

ACKNOWLEDGEMENTS

This work was supported by EURATOM and carried out within the framework of the European Fusion Development Agreement. The views and opinions expressed herein do not necessarily reflect those of the European Commission. The authors are thankful to D.Harting for helpful discussions.

REFERENCES

- [1]. M.F. Stamp et al., *Journal of Nuclear Materials* **415** (2011) S170–S173
- [2]. D.Borodin et al., *Physica Scripta* **T145** (2011) 014008
- [3]. W. Eckstein (2007) *Topics in Applied Physics*, 110, pp. 33-187; doi: 10.1007/978-3-540-44502-9-3
- [4]. D. Borodin et al., *Contribution to Plasma Physics* 50 (3–5) (2010) 432–438.
- [5]. Summers HP, 2004 *The ADAS User Manual* version 2.6; <http://adas.phys.strath.ac.uk>
- [6]. C.Björkas, these proceedings
- [7]. G F Matthews et al., *Physica Scripta* **T145** (2011) 014001
- [8]. D. Nishijima et al., *Journal of Nuclear Materials* **390-391** (2009) 132-135
- [9]. R. Behrisch and W. Eckstein “Sputtering by Particle Bombardment: Experiments and Computer Calculations from Threshold to MeV Energies”, Springer, 2007, Berlin

- [10]. J.Miettunen et al., these proceedings
 [11]. A. Kirschner et al., Physica Scripta **T128** (2009)
 [12]. A Pospieszczyk et al., Journal of Physics B: Atomic Molecular and Optical Physics **43** (2010) 144017
 [13]. X. Bonnin et al., EFDA report, EFDA-JET-CP(05)02-19; <http://www.iop.org/Jet/fulltext/EFDC050219.pdf>
 [14]. C.Silva et al., these proceedings

	q	E_{th}	μ	λ
“ERO-max”, D on Be	0.1386	5.9907	0.6206	0.8059
“ERO-min”, D on Be	0.0323	9.9686	0.7558	1.1874
“ERO-max”, Be on Be	0.8241	16.9689	0.8241	2.0334
“ERO-min”, Be on Be	0.1865	19.5634	0.9113	1.4486

Table 1. Fitting parameters for Be sputtering yield fit [3] used in ERO calculations as low and high limit estimates (normal incidence).

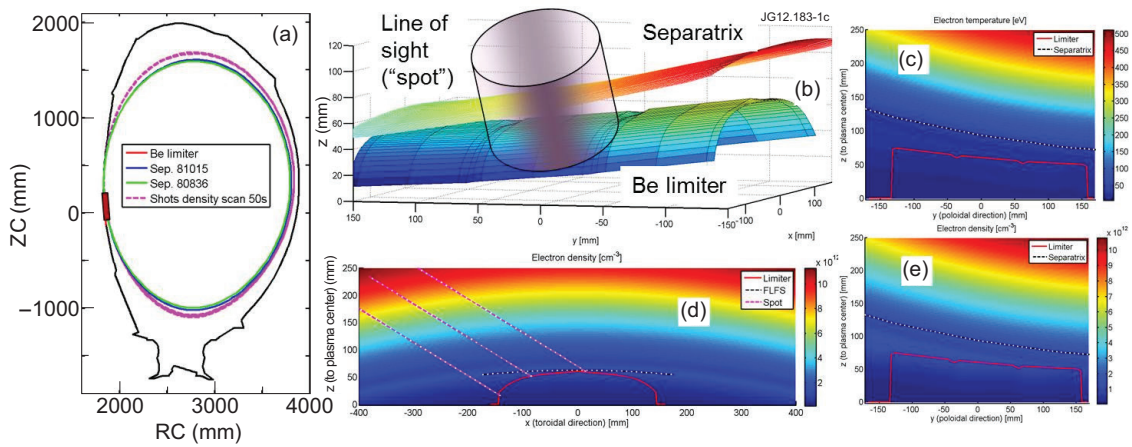


Figure 1: General experiment geometry. a) Poloidal position of the Be limiter tile. b) 3D limiter shape and the cylindrical light-integration volume along the line of sight of the spectroscopic system. c) Poloidal cross-section of electron temperature. d), e) Poloidal and toroidal cross-section of electron density. The ERO Cartesian coordinate system (x , y , z) is used (sec. 3); y is parallel to torus axis (JET coordinate “ ZC ”); x is in toroidal direction at the limiter central tip.

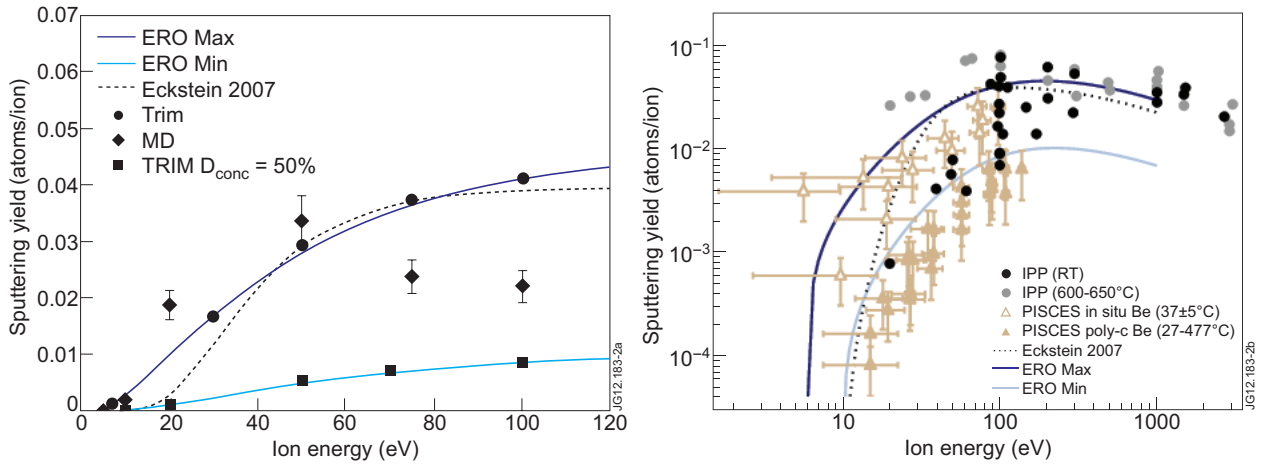


Figure 2: Erosion yield estimates “ERO-min” and “ERO-max” for Be sputtering by D used in the simulations (normal incidence part). Simulated data used for deduced fits (left) and comparison with various empiric data [8,9].

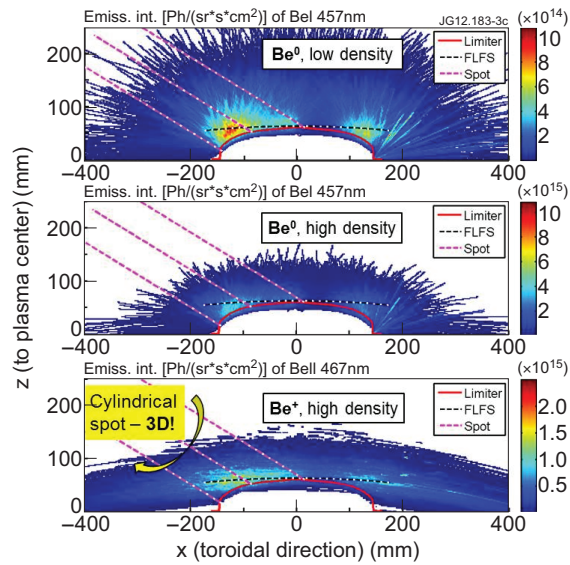


Figure 3: Emission patterns simulated by ERO for neutral (at “low line-integrated density” $4 \times 10^{19} \text{m}^{-2}$ and “high line-integrated density” $4 \times 10^{19} \text{m}^{-2}$) and ionized Be (for “high line-integrated density”). The observation system integration volume is indicated.

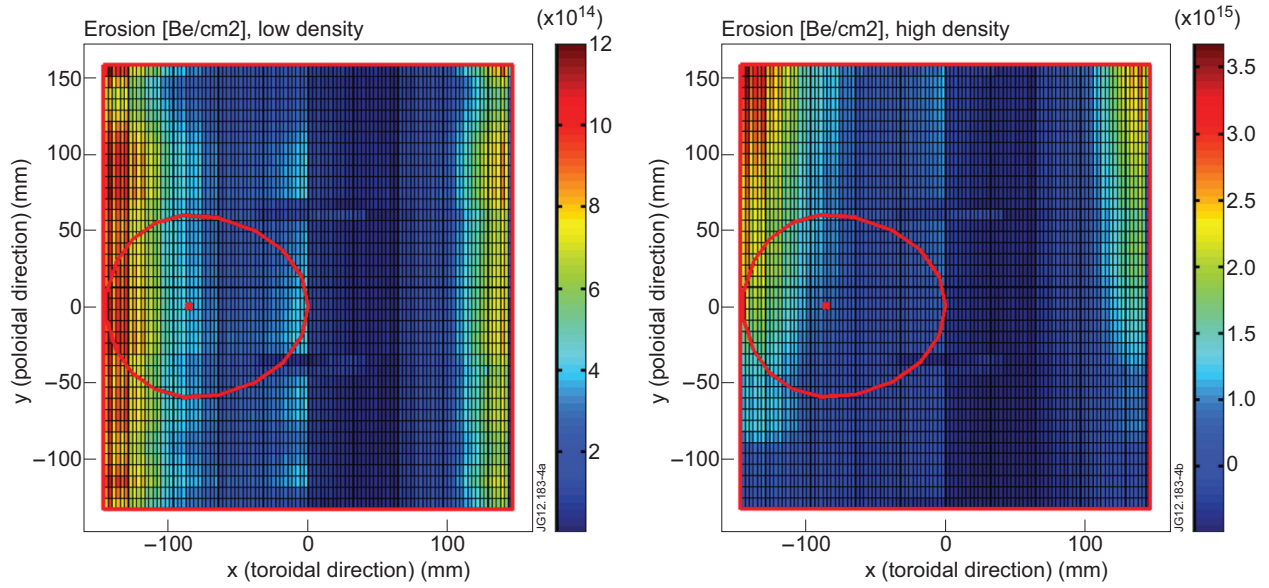


Figure 4: Erosion patterns for 1s long plasma exposure (low and high density as on fig. 3) along the Be shaped limiter surface simulated by ERO. Local transport determines the fraction of eroded Be coming into the marked spot location.

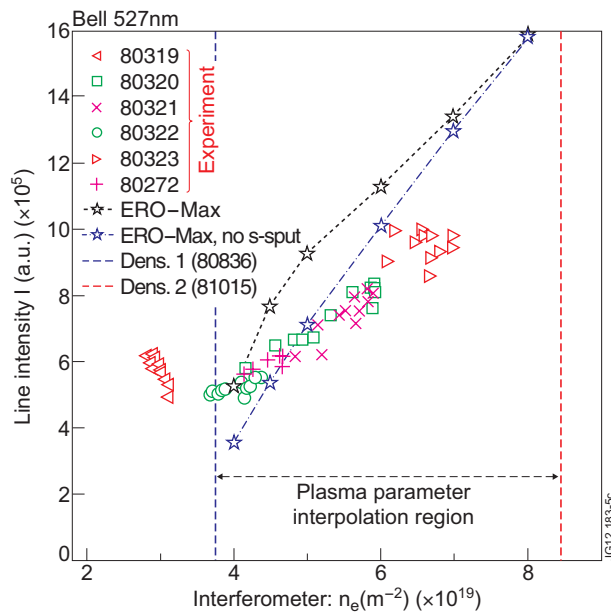


Figure 5: Total intensity of BeII 467nm line inside the spot. Experimental data obtained during several JET discharges are depicted alongside ERO simulations (also “no s-sput” – without self-sputtering by Be plasma impurity). The densities for which 2D-mapping of plasma parameters were made (limiting interpolation range) are indicated.

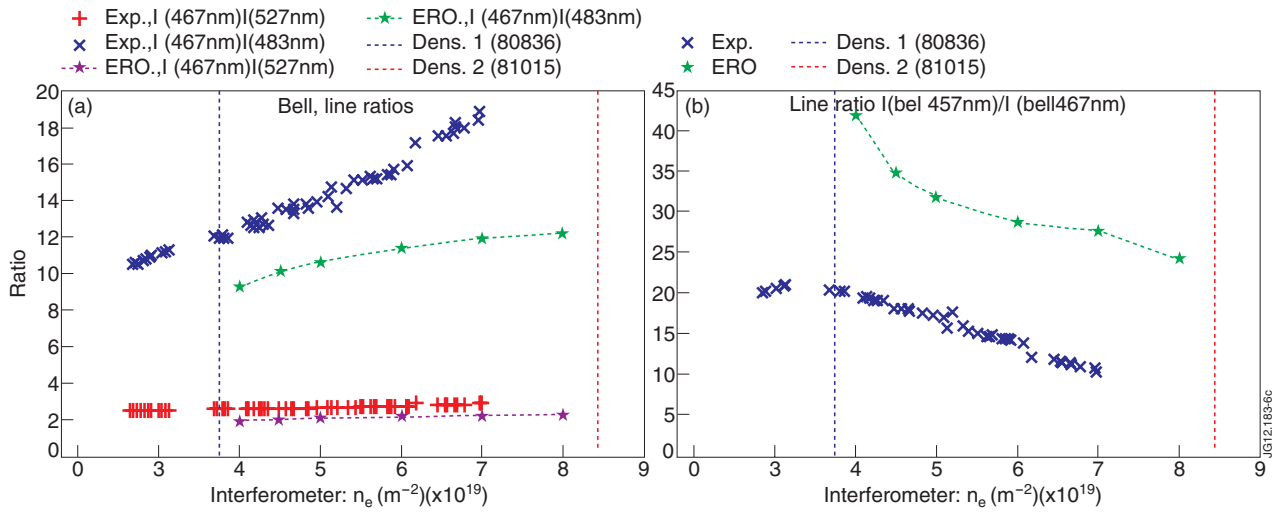


Figure 6: Absolute line ratios inside BeII (left) and between BeI and BeII lines during plasma density scan illustrating agreement between the experiment and the ERO simulations.